iScience

CellPress

Article

S-Adenosylmethionine Synthetase Is Required for Cell Growth, Maintenance of G0 Phase, and Termination of Quiescence in Fission Yeast

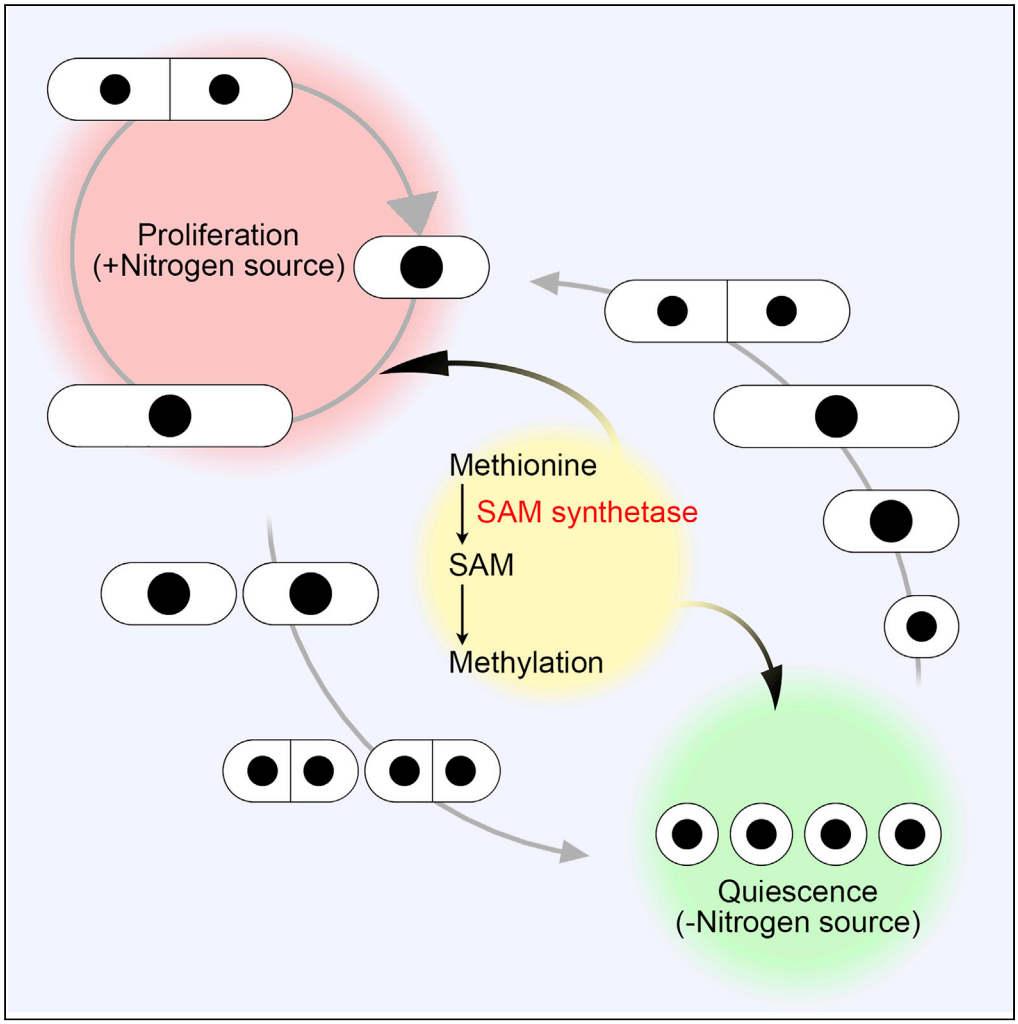

Takeshi Hayashi, Takayuki Teruya, Romanas Chaleckis, Susumu Morigasaki, Mitsuhiro Yanagida

myanagid@gmail.com

HIGHLIGHTS

Fission yeast temperature-sensitive mutant strains of SAM synthetase were isolated

SAM synthetase is essential for both proliferation and quiescence

SAM synthetase mutants show pleiotropic drug sensitivities

Extensive changes occur in the metabolic profiles of SAM synthetase mutants

Hayashi et al., iScience 5, 38–51
July 27, 2018 © 2018 The Author(s).
https://doi.org/10.1016/j.isci.2018.06.011

iScience

CellPress

Article

S-Adenosylmethionine Synthetase Is Required for Cell Growth, Maintenance of G0 Phase, and Termination of Quiescence in Fission Yeast

Takeshi Hayashi,[1] Takayuki Teruya,[1] Romanas Chaleckis,[1,2] Susumu Morigasaki,[1] and Mitsuhiro Yanagida[1,3,*]

SUMMARY

S-adenosylmethionine is an important compound, because it serves as the methyl donor in most methyl transfer reactions, including methylation of proteins, nucleic acids, and lipids. However, cellular defects in the genetic disruption of S-adenosylmethionine synthesis are not well understood. Here, we report the isolation and characterization of temperature-sensitive mutants of fission yeast S-adenosylmethionine synthetase (Sam1). Levels of S-adenosylmethionine and methylated histone H3 were greatly diminished in *sam1* mutants. *sam1* mutants stopped proliferating in vegetative culture and arrested specifically in G2 phase without cell elongation. Furthermore, *sam1* mutants lost viability during nitrogen starvation-induced G0 phase quiescence. After release from the G0 state, *sam1* mutants could neither increase in cell size nor re-initiate DNA replication in the rich medium. Sam1 is thus required for cell growth and proliferation, and maintenance of and exit from quiescence. *sam1* mutants lead to broad cellular and drug response defects, as expected, since *S. pombe* contains more than 90 S-adenosylmethionine-dependent methyltransferases.

INTRODUCTION

Methylation, the transfer of a methyl group from one molecule to another, is one of the most important and universal biochemical reactions in cells, where it is involved in numerous cellular processes, such as transcriptional control, lipid metabolism, and signal transduction. The diversity of functions involving methylation is sustained by numerous methyltransferases that are present in all living organisms. Although a broad range of molecules including proteins, nucleic acids, lipids, and cellular metabolites can be substrates for methyltransferases, almost all methyltransferases use S-adenosylmethionine (SAM, also known as SAMe or AdoMet) as the common methyl donor (Chiang et al., 1996). SAM is also required in other important processes, including synthesis of polyamines (Fontecave et al., 2004), which are essential for various cellular functions affecting growth and development (Pegg and Casero, 2011). Thus, SAM is the most versatile biomolecule, second to ATP, in biochemical processes (Loenen, 2006).

SAM is synthesized from methionine and ATP by SAM synthetase (also known as methionine adenosyltransferase [MAT]), and converted to S-adenosylhomocysteine (SAH) via methyl transfer reactions. Then it is regenerated via the methionine cycle (Figure 1A). SAM synthetases are highly conserved among diverse organisms and have been extensively studied in bacteria (Wei and Newman, 2002), fungi (Gerke et al., 2012; Hilti et al., 2000; Thomas and Surdin-Kerjan, 1991), plants (Li et al., 2011; Shen et al., 2002), and animals, including humans (Ding et al., 2015; Obata and Miura, 2015; Ramani and Lu, 2017). However, genetic analyses of SAM synthesis disruption are scarce, because multiple genes encode SAM synthetases in the majority of eukaryotic organisms, including the budding yeast, *Saccharomyces cerevisiae*.

The fission yeast, *Schizosaccharomyces pombe*, is an excellent model organism to study eukaryotic molecular and cellular biology (Hoffman et al., 2015; Yanagida, 2002). *S. pombe* has more than 90 genes predicted to encode SAM-dependent methyltransferases, according to PomBase (Wood et al., 2012). The physiological roles of methylation have been investigated by inactivating specific methyltransferases involved in a wide range of cellular processes, such as biomolecule synthesis (Hayashi et al., 2014a; Iwaki et al., 2008; Kanipes et al., 1998; Pluskal et al., 2014), ribosome function (Bachand and Silver, 2004; Shirai et al., 2010), transcriptional control (Ekwall and Ruusala, 1994; Morris et al., 2005; Thon et al., 1994), and DNA damage response (Sanders et al., 2004). However, cellular defects in the genetic control of SAM synthesis are not well understood. *S. pombe* possesses a single gene for SAM synthetase, *sam1*$^{+}$, which is

[1]G0 Cell Unit, Okinawa Institute of Science and Technology Graduate University, Onna-son, Okinawa 904-0495, Japan

[2]Present address: Gunma University Initiative for Advanced Research (GIAR), Gunma University, Gunma 371-8511, Japan

[3]Lead Contact

*Correspondence: myanagid@gmail.com

https://doi.org/10.1016/j.isci.2018.06.011

This is an open access article under the CC BY-NC-ND license (http://creativecommons.org/licenses/by-nc-nd/4.0/).

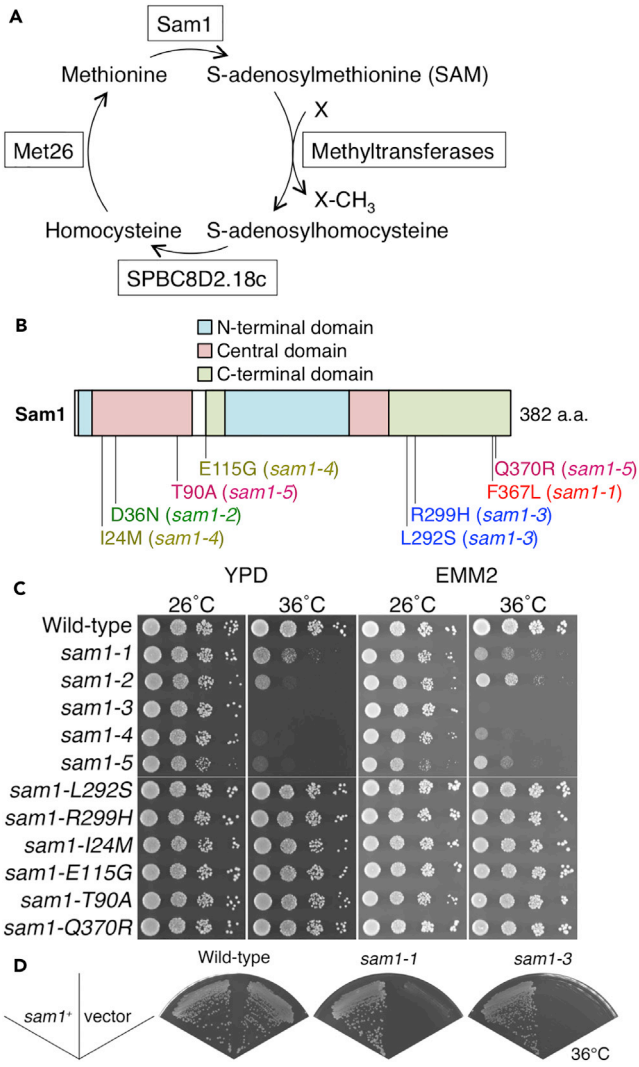

Figure 1. Isolation of Temperature-Sensitive Mutants of *sam1*

(A) Schematic illustration of the methionine cycle in the fission yeast, *S. pombe*. Sam1, SAM synthetase; SPBC8D2.18c, adenosylhomocysteinase (AHCY); Met26, methionine synthase.

(B) Locations of mutations of *sam1* mutants determined by nucleotide sequencing in domain architecture based on the three-dimensional structure.

(C) *sam1-1*–*sam1-5* mutants failed to produce colonies at 36°C on both rich YPD and synthetic minimal EMM2 plates, whereas *sam1* mutants containing one of two amino acid substitutions in *sam1-3*–*sam1-5* mutants produced colonies at 36°C.

(D) The colony formation defects of *sam1-1* and *sam1-3* at 36°C were rescued by pREP41 plasmid carrying the *sam1*$^+$ gene. Cells were streaked onto EMM2 plates in the absence of thiamine to induce the expression of *sam1*$^+$.

See also Figures S1 and S2.

essential for cell viability, and low expression of *sam1*$^+$ affects growth, mating, and sporulation (Hilti et al., 2000).

In this study, we report isolation by PCR random mutagenesis and characterization of temperature-sensitive (ts) mutant strains of fission yeast SAM synthetase and demonstrate that *sam1*$^+$ is a super-housekeeping (SHK) gene, essential for both proliferation and quiescence (Sajiki et al., 2009). Mutations in the *sam1* gene block cell growth and cell cycle progression in vegetative culture and also cause failure to exit from nitrogen starvation-induced G0 quiescence. Furthermore, *sam1* mutants lose cell viability during G0 quiescence.

RESULTS

Isolation of Temperature-Sensitive Mutants of the *sam1* Gene

Because the *sam1*$^+$ gene is essential for cell viability (Hilti et al., 2000; Kim et al., 2010), we examined the effects of SAM limitation on cellular functions by isolating *S. pombe* ts mutants of SAM synthetase Sam1. To obtain ts mutants of the *sam1*$^+$ gene, we employed a PCR-based random mutagenesis screen (Hayashi et al., 2014b) (Figure S1). The *sam1* DNA fragment, in which the hygromycin-resistance-encoding marker gene, *hph*, was inserted just downstream of the stop codon of the *sam1*$^+$ gene open reading frame, was amplified by PCR under error-prone conditions, containing increased $MgCl_2$ (Eckert and Kunkel, 1990). Mutagenized DNA fragments were introduced into wild-type (WT) cells for replacement of the chromosomal *sam1*$^+$ gene with the mutated gene by homologous recombination. Hygromycin-resistant transformants were selected at 26°C and then tested for colony formation at 36°C on rich YPD medium plates. After confirmation of linkage of the ts phenotype to the hygromycin-resistant phenotype, five ts mutant strains of the *sam1* gene were obtained and designated *sam1-1* to *sam1-5*.

We then identified mutation sites in the *sam1* gene of the *sam1* ts mutants. *sam1-1* and *sam1-2* contained single amino acid substitutions (F367L and D36N, respectively), whereas *sam1-3*, *sam1-4*, and *sam1-5* contained two amino acid substitutions (L292S R299H, I24M E115G, and T90A Q370R, respectively) in the *sam1* gene (Figure 1B). All mutation sites except for Q370 are conserved among humans, rats, and fission yeast. Based on the three-dimensional structure of the rat ortholog of Sam1 (González et al., 2003), no mutations were found to locate near the binding site of the substrates, ATP and methionine (Figure S2). To identify the mutations responsible for the ts phenotype, we introduced one of the five mutant sequences (*sam1-1*–*sam1-5*) or one of two amino acid substitutions in *sam1-3*–*sam1-5* mutants into the WT genome using linearized plasmids carrying the hygromycin resistance marker. The resulting transformants, containing chromosomal gene replacements with the *sam1-1*–*sam1-5* mutant genes, showed the ts phenotype on both rich YPD and synthetic minimal EMM2 plates, whereas the transformants containing one of two amino acid substitutions in *sam1-3*–*sam1-5* mutants did not show the ts phenotype (Figure 1C). In conclusion, *sam1* gene mutations in the mutants caused the ts phenotype and both the amino acid substitutions in *sam1-3*–*sam1-5* were necessary for the ts phenotype. Since *sam1-3* showed the most severe growth defects and *sam1-1* showed a moderate ts phenotype at 36°C on YPD plates (Figure 1C), *sam1-1* and *sam1-3* were used for further investigation. It was confirmed that the colony formation defects of *sam1-1* and *sam1-3* at 36°C were rescued by plasmid carrying the *sam1*$^+$ gene (Figure 1D).

Defective SAM Synthetase in *sam1* Mutant Cells

To detect Sam1 protein, polyclonal antibodies against a mixture of two peptides (I^{77}GYDDSEKGFDYKTC^{91} and N^{320}TYGTSSKTSAELV^{333}) of *S. pombe* Sam1 were raised and used for immunoblots after affinity purification. We validated the specificity of the α-Sam1 antibodies by detecting a single band at the expected molecular weight of ~42 kD in immunoblots of WT cell extracts (no tag, Figure 2A). The assignment of the band was confirmed using extracts of Sam1-FLAG cells in which the chromosomal *sam1*$^+$ gene was replaced with the *sam1*$^+$*-FLAG* gene. The band detected by immunoblot using α-Sam1 antibodies was shifted to ~45 kD in extracts of Sam1-FLAG cells (Figure 2A). Untagged Sam1 was not detected by α-FLAG antibody. Thus, polyclonal antibodies against Sam1 specifically detected Sam1 protein in cell extracts. We then compared protein levels of Sam1 in WT and *sam1* mutant cells cultured at 36°C for 0–6 hr in rich YPD medium. Sam1 mutant proteins of *sam1-1* and *sam1-3* were diminished, compared with WT, even at the permissive temperature of 26°C (0 hr, Figure 2B), and further decreased at 36°C. These results suggest that *sam1-1* and *sam1-3* mutants are loss-of-function mutants of SAM synthetase Sam1, partly due to the decreased protein level.

If *sam1-1* and *sam1-3* mutants are indeed defective in SAM synthetic activity, SAM should be decreased in the mutant cells. We employed metabolomic analysis using liquid chromatography-mass spectrometry to assay the levels of SAM and related metabolites in extracts of WT and *sam1* mutant cells grown in rich YPD medium. WT and *sam1* mutant cells were grown at 26°C and then shifted to 36°C for 0–24 hr. Levels of SAM detected in *sam1-1* and *sam1-3* cell extracts were rather low, even at the permissive temperature of 26°C (0 hr, Figure 2C), and further decreased at 36°C, whereas the high level of SAM in WT was maintained at 36°C for 0–24 hr (Figure 2C). Similar results were obtained for SAH, a by-product of SAM-dependent methyl transfer reactions (Figure 2D). Levels of methionine, a substrate of Sam1 enzyme, were decreased in WT cells, but not in *sam1* mutants at 36°C (Figure 2E). These results strongly support the notion that SAM synthesis was defective in *sam1-1* and *sam1-3* mutant cells.

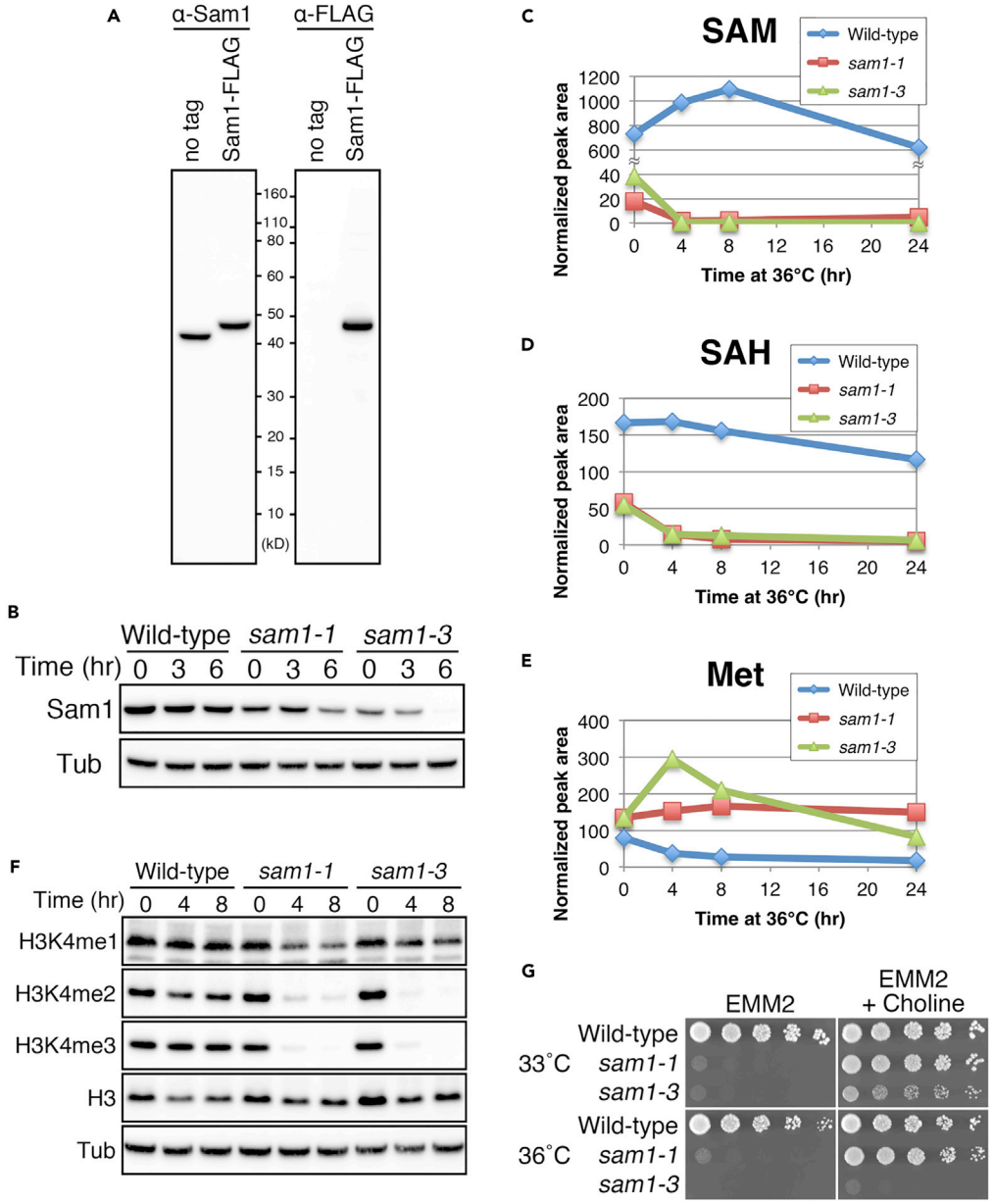

Figure 2. *sam1* Mutants Are Defective in SAM Synthesis and Histone H3K4 Methylation, and Are Rescued by Choline

(A) Immunoblot of extracts of WT (no tag) and Sam1-FLAG cells using affinity-purified anti-Sam1 and anti-FLAG antibodies.

(B) Levels of mutant Sam1 proteins were diminished. Immunoblotting was done using antibodies against Sam1 to detect Sam1 protein in the extracts of WT, *sam1-1*, and *sam1-3* cells cultured at 36°C for 0–6 hr in rich YPD medium. Antibody against α-tubulin (Tub) was used as the loading control.

(C–E) The time course change of the normalized peak areas of SAM and related metabolites. Metabolites were extracted from WT and *sam1* mutant cells cultured at 36°C for 0–24 hr in rich YPD medium and analyzed. Normalized peak areas of the following metabolites are shown: (C) S-adenosylmethionine (SAM); (D) S-adenosylhomocysteine (SAH); (E) methionine (Met).

(F) Levels of methylated histone H3 K4 in WT, *sam1-1*, and *sam1-3* cells. WT, *sam1-1*, and *sam1-3* cells were cultured at 36°C for 0–8 hr in rich YPD medium. Antibodies against histone H3 and mono-, di-, and trimethylated H3K4 (H3K4me1, H3K4me2, and H3K4me3, respectively) were used to detect the total H3 and methylated H3K4.

(G) Cells were diluted serially 10-fold, spotted onto EMM2 or EMM2 containing 2 mM choline chloride, and incubated at 30°C, 33°C, or 36°C for 3 days.

Impairment of Methylation Reactions in *sam1* Mutants

Because the levels of SAM, a universal methyl group donor, were greatly decreased in *sam1* mutant cells, we next investigated histone methylation in *sam1* mutant cells. WT and *sam1* mutant cells were shifted from 26°C to 36°C for 0–8 hr, and immunoblot analysis was carried out using three antibodies specific to mono-, di-, and trimethylated lysine 4 of histone H3 (H3K4me1, H3K4me2, and H3K4me3, respectively). In *sam1-1* and *sam1-3* mutant cells, the levels of H3K4me2 and H3K4me3 were greatly decreased after the shift to 36°C, whereas only a slight decrease was observed in H3K4me1 (Figure 2F). These results suggested that a global change of histone methylation was caused by mutations of SAM synthetase and that levels of di- and trimethylated Lys4 of histone H3 were more susceptible to SAM deficiency.

Many eukaryotes, including *S. pombe*, produce phosphatidylcholine (PC) via two pathways. One is methylation of phosphatidylethanolamine, a major methylation target in mammals and budding yeast (Noga et al., 2003; Stead et al., 2006; Ye et al., 2017). Another PC biosynthetic pathway is the CDP-choline pathway, which is independent of methylation and requires choline (Kanipes et al., 1998; Kent, 1995). We presumed that exogenous choline relieves the ts phenotype of *sam1* mutants by rescuing the PC synthesis defect. As expected, colony formation of *sam1-1* and *sam1-3* at 33–36°C and 33°C, respectively, on EMM2 agar plates was rescued by adding choline (Figure 2G). These results strongly suggested that the *sam1* mutations impaired cellular methylation reactions.

Diminished Cell Growth and Cell-Cycle Arrest in G2 Phase Occur in *sam1* Mutants

We examined the cellular phenotypes of *sam1-1* and *sam1-3* mutant cells at the restrictive temperature (36°C). WT and *sam1* mutant cells were grown at 26°C and then shifted to 36°C in rich YPD medium. The cell number increase of *sam1* mutants stopped after one or two cell divisions at 36°C (Figure 3A), although the high viability of mutant cells was still maintained after 8 hr (Figure 3B). Since fluorescence microscopic observation of DNA-specific probe DAPI -stained cells demonstrated that most *sam1-1* and *sam1-3* cells were mononucleate 8 hr after the shift to 36°C (Figure 3C), the *sam1* mutants probably arrest the cell cycle at the higher temperature. The length of *sam1* mutant cells did not increase significantly compared with WT after the shift to 36°C. Average cell lengths of WT, *sam1-1*, and *sam1-3* were 11.6 $\pm$ 2.3, 11.5 $\pm$ 2.4, and 11.8 $\pm$ 2.4 μm, respectively, after 8 hr at 36°C (Figure 3D), suggesting that cell growth (i.e., the extension of cell length) halted at 36°C in *sam1* mutant cells, unlike *cdc* mutants that develop extremely elongate cells because of growth without cell division (Nurse et al., 1976).

To monitor cell cycle progression in WT and *sam1* mutant cells at 36°C, we measured the septation index (percentage of cells with a septum), the cellular DNA content, and the spindle index (percentage of cells with mitotic spindle). The septation index was maintained at ~12% in WT cells, whereas it dropped to 0.8% 4 hr after the shift to 36°C in *sam1-3* mutant cells and to 1.2% at 8 hr in *sam1-1* mutant cells (Figure 3E). These results indicate that *sam1* mutant cells were arrested before the onset of cytokinesis. In cellular DNA content analysis by fluorescence-activated cell sorting (FACS), a single peak appeared before the shift to 36°C (0 hr) in WT and *sam1* mutants, meaning 2C DNA content, because most vegetatively growing *S. pombe* cells are mononucleate in post-replicative (G2) phase and pre-replicative nuclei exist in binucleate cells (Figure 3F). After the shift to 36°C (2–8 hr), only one peak at the 2C DNA content was still present in *sam1-1* and *sam1-3* mutants, like WT cells, indicating that cell-cycle arrest in *sam1* mutants at the restrictive temperature occurred after completion of DNA replication. The spindle index was measured using WT and *sam1* mutant strains expressing α-tubulin-GFP and Cut11-mCherry, which visualized spindle microtubules and the nuclear envelope, respectively (Figures 3G and 3H). The spindle index was maintained around 8%–10% in WT cells at 36°C for 0–6 hr, whereas it dropped to 0% at 4 hr after the shift to 36°C in *sam1-3* mutant cells and to 0.4% at 6 hr in *sam1-1* mutant cells (Figure 3G), indicating that *sam1* mutant cells arrested before the onset of M phase. Consequently, *sam1* mutant cells arrest specifically in G2 phase at the restrictive temperature in rich YPD medium.

sam1 Mutant Cells Lose Cell Viability in the Maintenance of G0 Phase Induced by Nitrogen Starvation

To determine the capacity of *sam1* mutants to maintain viability in the nitrogen starvation-induced quiescent G0 phase, we monitored cell viability under nitrogen starvation (Sajiki et al., 2009; Shimanuki et al., 2007). WT and *sam1* mutant cells first grown in EMM2 medium were transferred to the nitrogen-deficient EMM2−N at 26°C for 24 hr to enter a quiescent G0 state. After 24 hr, the cell number increase in the *sam1-1* mutant was only 2.4-fold, whereas that in WT and *sam1-3* mutants was around 3.6-fold (Figure 4A). FACS

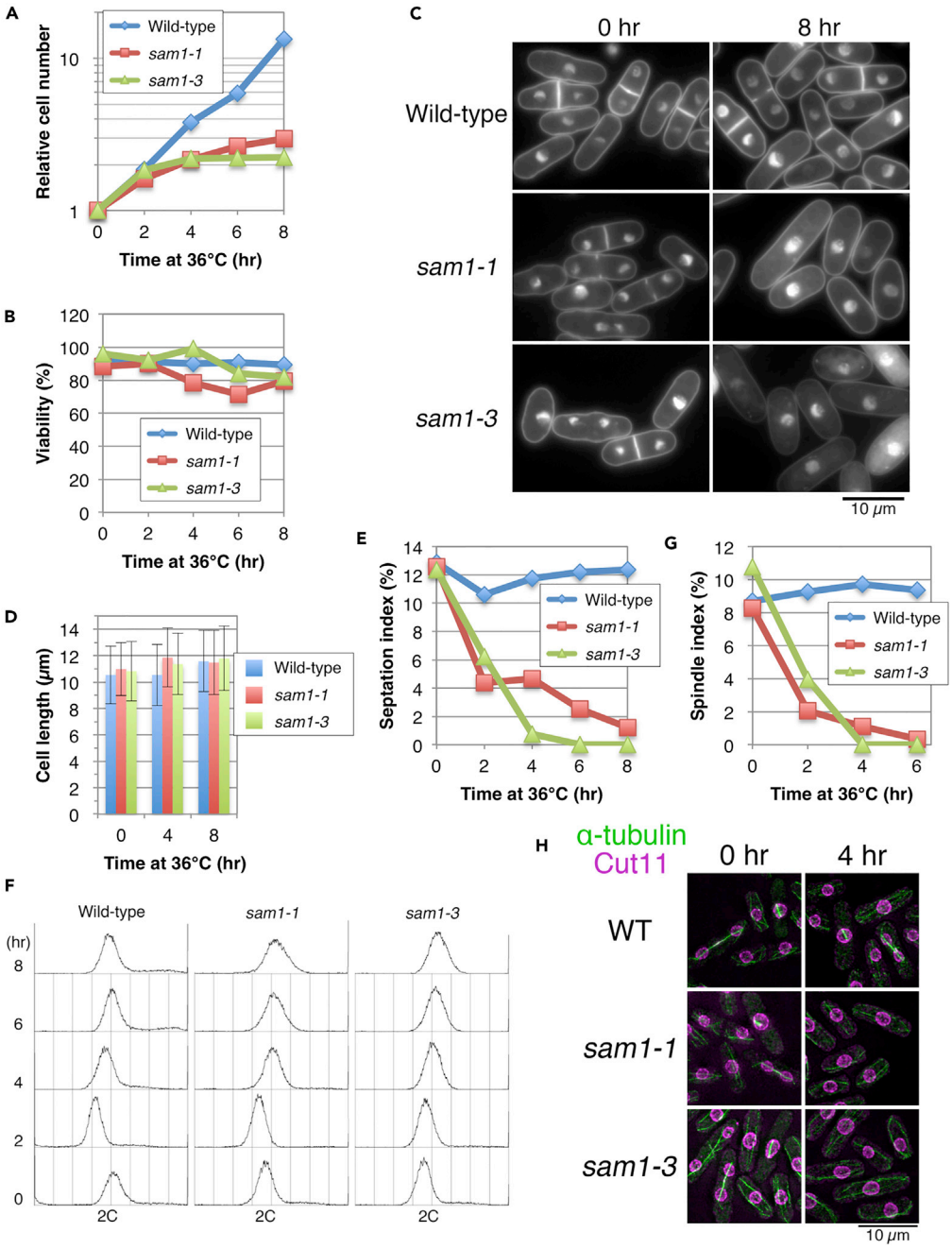

Figure 3. Diminished Cell Growth and Cell-Cycle Arrest in G2 Phase Occur in *sam1* Mutants

(A–F) WT, *sam1-1*, and *sam1-3* cells were grown at 26°C in rich YPD medium and then shifted to 36°C. The cell number increase (A), the viability change (B), fluorescence microscopic images of DAPI-stained cells (C), the average cell length with standard deviations (D), the proportion of cells with a septum (septation index) (E), and the distributions of cellular DNA content (F) are shown. Cell viability was measured by plating cells onto YPD agar and counting the number of colonies formed after incubation at 26°C.

(G and H) Time courses of changes in spindle index (G) and fluorescence microscopic images (H) of WT, *sam1-1*, and *sam1-3* cells expressing GFP-fused α-tubulin and mCherry-fused Cut11 after the shift from 26°C to 36°C in YPD medium. GFP and mCherry fluorescence is shown in green and magenta, respectively.

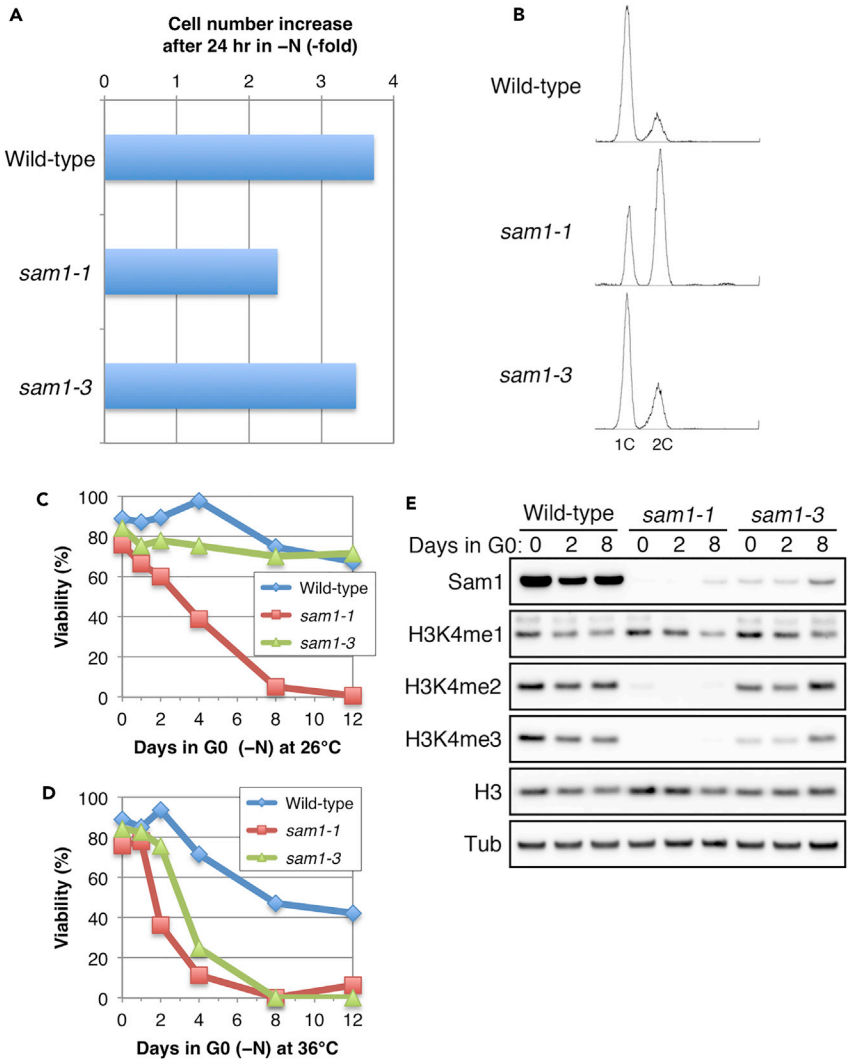

Figure 4. *sam1* Mutant Cells Lose Cell Viability in the Maintenance of Nitrogen Starvation-Induced G0 Phase

(A and B) WT, *sam1-1*, and *sam1-3* cells were brought into the G0 quiescent state at 26°C under nitrogen-deficient medium, EMM2−N for 24 hr. Increase in cell number as the fold increase (A) and the distribution of cellular DNA content (B) after 24 hr in EMM2−N medium at 26°C are shown.

(C and D) Resulting G0 quiescent cultures were kept at 26°C (C) or shifted to 36°C (D) for 12 days. The cell viability percentages were scored at different time points (days). *sam1-1* mutant cells lost cell viability both at 26°C and 36°C, whereas *sam1-3* mutant cells lost cell viability only at 36°C.

(E) Levels of Sam1 and methylated histone H3 K4 in WT, *sam1-1*, and *sam1-3* cells in nitrogen starvation-induced G0 phase at 26°C. WT, *sam1-1*, and *sam1-3* cells were brought into the G0 quiescent state under nitrogen-deficient medium, EMM2−N for 24 hr (day 0), and further incubated at 26°C for 8 days. Immunoblotting was done using antibodies against Sam1, α-tubulin (Tub), histone H3, and mono-, di- and trimethylated H3K4 (H3K4me1, H3K4me2, and H3K4me3, respectively).

analysis revealed that ~80% of WT and *sam1-3* cells contained 1C DNA, whereas 1C DNA-containing *sam1-1* cells accounted for only ~40% (Figure 4B). These results indicated that the *sam1-1* mutant was somewhat defective in pre-quiescence division under nitrogen starvation at 26°C. Nitrogen starvation-induced quiescent G0 cells were further cultivated at either 26°C or 36°C for 12 days. G0-arrested WT and *sam1-3* cells maintained high viability at 26°C, whereas G0-arrested *sam1-1* cells gradually lost viability even at 26°C (Figure 4C). At 36°C, the viability of *sam1-1* and *sam1-3* decreased to <25% after 4 days and to <0.3% after 8 days, whereas the viability of WT was ~40% after 12 days at 36°C (Figure 4D). Together, functional Sam1 is required for the maintenance of G0 phase under nitrogen starvation.

Since *sam1-1* lost viability at 26°C during nitrogen starvation, whereas *sam1-3* did not, we compared the mutant Sam1 protein abundance in *sam1-1* with that in *sam1-3* mutants in G0 phase 0–8 days after culture for 24-hr quiescence entry in the EMM2−N medium. Although the Sam1 proteins of both *sam1-1* and *sam1-3* were diminished compared with that of WT under nitrogen starvation at 26°C, the mutant Sam1 protein level was lower in *sam1-1* than in *sam1-3* (Figure 4E). In addition, levels of H3K4me2 and H3K4me3 were already greatly decreased in *sam1-1* at day 0 in G0 (24 hr after nitrogen removal), whereas only a slight decrease of H3K4me3 was observed in *sam1-3* (Figure 4E). These results are consistent with the data in Figure 4C.

sam1 Mutant Cells Fail to Exit from Nitrogen-Starved Arrest

We next addressed the question of whether *sam1* mutant cells could exit from a nitrogen starvation-induced G0 state in which cells became small and contained pre-replicative 1C DNA (Su et al., 1996) (see also Figures 5C and 5D). WT and *sam1* mutants were first cultured in nitrogen-deficient medium, EMM2−N, at 26°C for 24 hr to induce G0 arrest, and then shifted to rich YPD medium for release from G0 arrest at 36°C. The cell number increase was completely blocked in *sam1-1* and *sam1-3* mutant cells after transfer to rich YPD medium at 36°C, whereas the cell number of WT started increasing after 6 hr (Figure 5A). However, the high viability of *sam1-1* and *sam1-3* mutant cells was maintained for 8 and 24 hr, respectively, in rich YPD medium at 36°C (Figure 5B). *sam1-1* and *sam1-3* mutant cells remained small and round even after 24 hr in rich YPD medium, whereas WT cells were a normal rod shape after 8 hr (Figure 5C), demonstrating that *sam1* mutants were unable to initiate cell growth at the restrictive temperature. FACS analysis showed that *sam1-1* and *sam1-3* mutant cells did not initiate DNA replication even after 24 hr, whereas WT cells completed DNA replication after 4 hr (Figure 5D). These results imply that Sam1 is necessary to initiate cell growth and DNA replication after the release from nitrogen starvation-induced G0 state.

Rapamycin Rescues *sam1* Mutants

The target of rapamycin (TOR) complex is the main regulator of cell growth and controls nutrient signaling pathways in eukaryotes (Kennedy and Lamming, 2016). We investigated the effect of rapamycin (an inhibitor of TOR kinase) on the ts phenotype of *sam1* mutants on rich YPD medium, as *sam1* mutants were defective in cell growth, as described above (Figures 3C and 5C). Rapamycin (0.1 μg/mL) rescued the growth defect of *sam1-1* mutant cells at 36°C and slightly suppressed the ts phenotype of *sam1-3* mutants at 33°C (Figure 6A), suggesting that reducing TOR activity relieved the growth defects of *sam1* mutants. Rapamycin may rescue *sam1* mutants in a way different from protein level restoration because the mutant Sam1 protein amount was not affected in *sam1-1* and *sam1-3* mutants by the addition of rapamycin at 26°C and 36°C (Figures 6B and 6C).

sam1 mutants were also defective in the maintenance of G0 phase induced by nitrogen starvation (Figures 4C and 4D), so we next tested whether rapamycin could rescue the viability loss of *sam1* mutants in G0 phase. Viability loss of *sam1-1* in G0 at 26°C was significantly suppressed by the addition of rapamycin, and the viability was >40% after 12 days, whereas the viability in the absence of rapamycin was ~3% after 8 days (Figure 6D). At 36°C, viability loss of *sam1-1* and *sam1-3* in G0 was delayed in the presence of rapamycin (Figure 6E). Thus, rapamycin rescued *sam1* mutants in both proliferative and quiescent phases.

sam1 Mutants Show Pleiotropic Drug Sensitivities

To search further the physiological roles of Sam1, we examined the drug sensitivity of *sam1* mutants. The response of *sam1-1* and *sam1-3* mutants to various stress agents is summarized in Table 1 (data are shown in Figure S3). Both mutants were sensitive to 25 mM nicotinamide, which inhibits class III histone deacetylases (HDACs) (Sauve et al., 2006), but not to 12.5 μg/mL trichostatin A (TSA), an inhibitor of class I and class II HDACs (Yoshida et al., 1995), at 30°C. These mutants were also sensitive to 4 μg/mL actinomycin D, an inhibitor of transcription (Bensaude, 2011), at 30°C. At 33°C, *sam1-1* was moderately sensitive to 4 mM hydroxyurea (HU, an inhibitor of DNA synthesis) (Singh and Xu, 2016), 8 μg/mL phleomycin (inducing double-strand DNA breaks) (Moore, 1988), and 4 μM camptothecin (CPT, an inhibitor of topoisomerase I that induces single-strand DNA breaks) (Pommier, 2006) and showed similar sensitivity to 100 J/m^2 UV irradiation (inducing the formation of thymine dimers) compared with the WT strain. No significant difference in the sensitivity of *sam1-3* to HU, phleomycin, CPT, and UV irradiation was observed, partly due to no growth at 33°C even without the treatments. Thus, *sam1* mutants showed hypersensitivity to a variety of drugs related to DNA damage and chromatin remodeling.

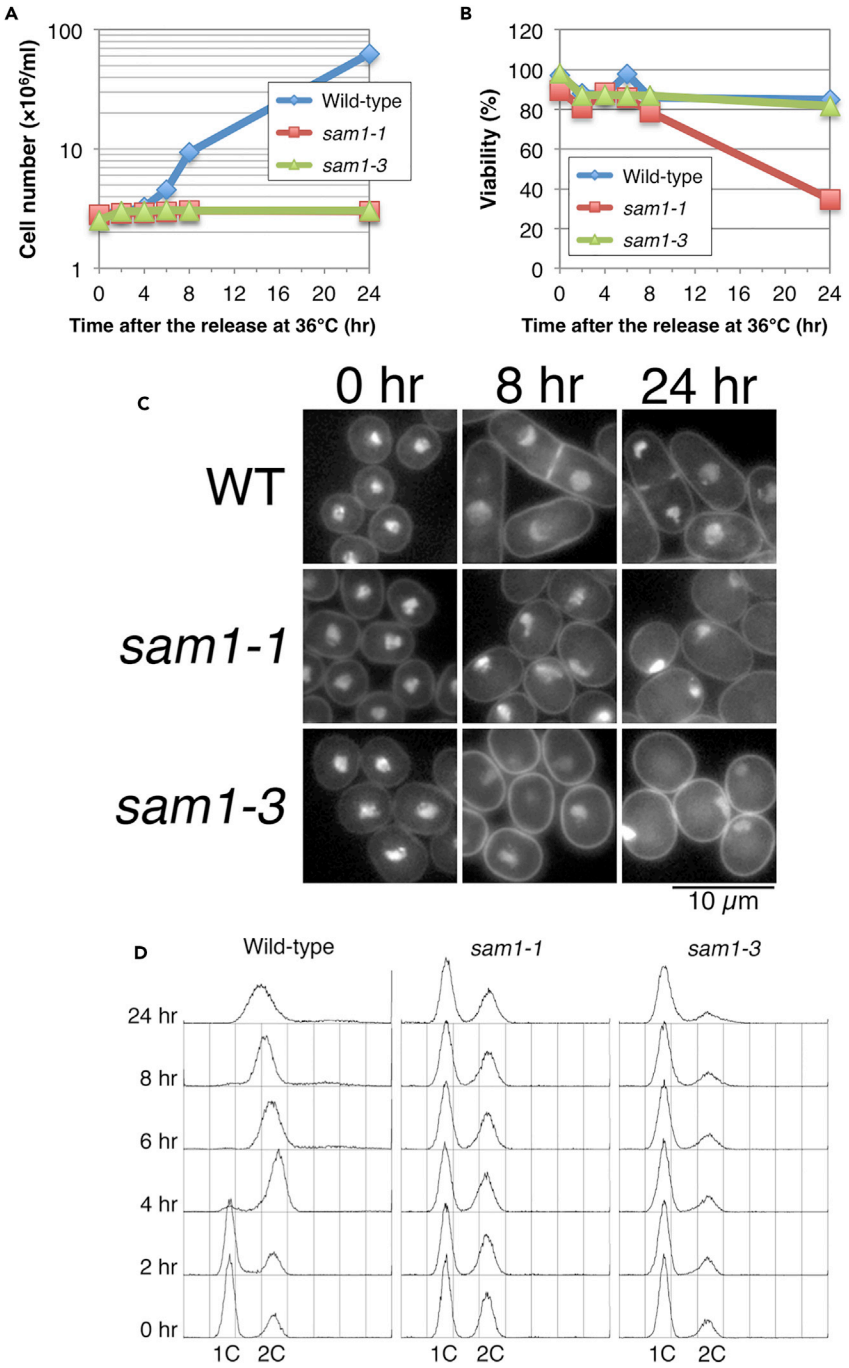

Figure 5. *sam1* Mutant Cells Fail to Exit from Nitrogen-Starved Arrest

(A–D) WT, *sam1-1*, and *sam1-3* were first cultured in nitrogen-deficient medium, EMM2−N, at 26°C for 24 hr to induce the G0 arrest. G0-arrested, small, round cells were then released to rich YPD medium at 36°C. The cell number increase (A), the viability change (B), fluorescence microscopic images of DAPI-stained cells (C), and the distributions of cellular DNA content (D) are shown.

Extensive Changes Occur in the Metabolic Profiles of *sam1* Mutants

We performed metabolomic analysis of WT and *sam1* mutant cells grown at 36°C for 8 hr in rich YPD medium to understand the impact of SAM limitation on metabolic homeostasis beyond the methionine cycle (Table S1). A comparison of WT with *sam1-1* is shown in a scatterplot (Figure 7A). The normalized peak area showed more than a 2-fold difference for 54 compounds (61%) out of 88 identified metabolites in comparison of WT

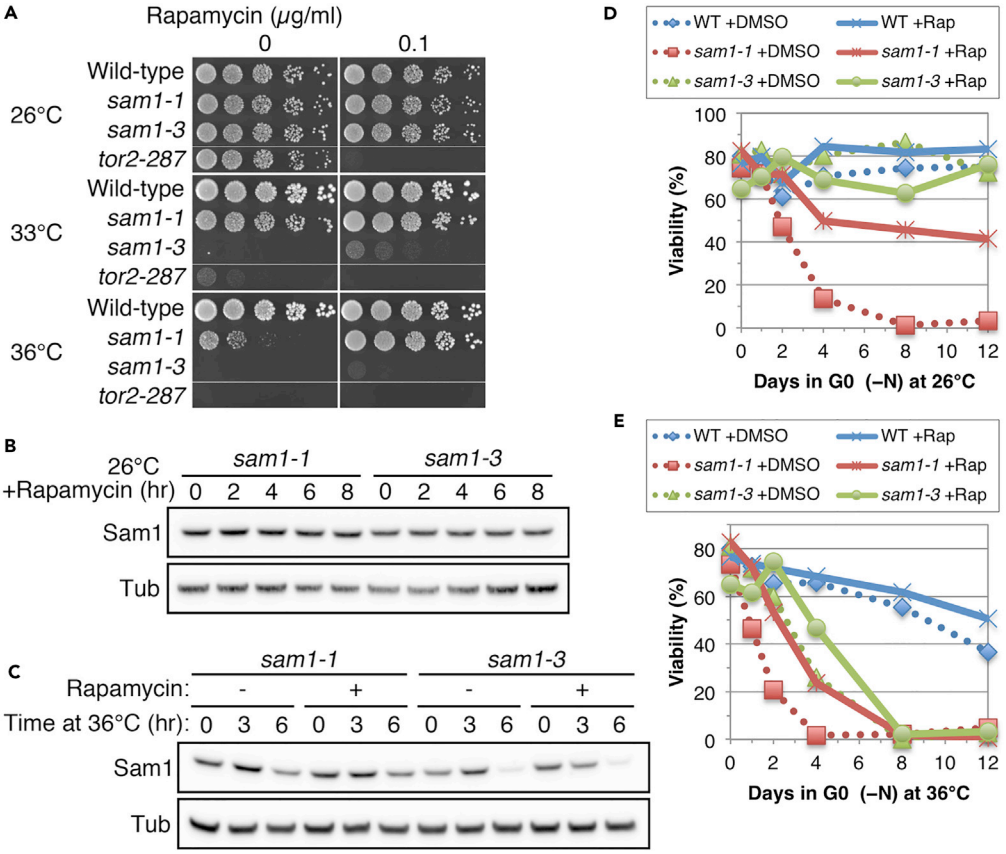

Figure 6. *sam1* Mutants Are Rescued by Rapamycin

(A) *sam1-1* and *sam1-3* were spotted on YPD plates in the presence or absence of rapamycin and then incubated at the indicated temperatures for 2–3 days. Wild-type and *tor2-287* (hypersensitive to rapamycin) (Hayashi et al., 2007) were used as controls.

(B) Levels of mutant Sam1 proteins in *sam1-1* and *sam1-3* cells in the presence of rapamycin at 26°C. *sam1-1* and *sam1-3* cells were cultured in YPD with 0.2 μg/mL rapamycin at 26°C. Immunoblotting was done using antibodies against Sam1 and α-tubulin (Tub).

(C) Levels of mutant Sam1 proteins in *sam1-1* and *sam1-3* cells in the presence or absence of rapamycin at 36°C. Rapamycin (0.2 μg/mL) or DMSO was added to YPD medium 2 hr before the shift up from 26°C to 36°C. Immunoblotting was done using antibodies against Sam1 and α-tubulin (Tub).

(D and E) Viability of WT, *sam1-1*, and *sam1-3* in nitrogen starvation-induced G0 phase with or without rapamycin. WT, *sam1-1*, and *sam1-3* cells were brought into the G0 quiescent state at 26°C under nitrogen-deficient medium with or without 0.2 μg/mL rapamycin (Rap) for 24 hr. Resulting G0 quiescent cultures were kept at 26°C (D) or shifted to 36°C (E) for 12 days. The cell viability percentages were scored at different time points (days).

with *sam1-1*, whereas only ~10% of the identified metabolites usually change more than 2-fold in comparisons of two independent experiments under identical conditions (Pluskal et al., 2010), indicating that the profile of metabolites was significantly altered in *sam1-1*. Similar results were obtained from comparisons of *sam1-3* with WT: the normalized peak areas of approximately 64% of identified metabolites had greater than a 2-fold change (Figure 7B). Beside the remarkable decrease of SAM and SAH described above (Figures 2C and 2D), eight compounds (phosphoribosyl pyrophosphate [PRPP], hercynylcysteine sulfoxide, CDP, UMP, adenine, UDP, sedoheptulose-7-phosphate, and pentose-phosphate) decreased over 10-fold in *sam1-1* and/or *sam1-3* mutant cells (Figure 7C). Hercynylcysteine sulfoxide is a precursor of ergothioneine, an antioxidant compound (Pluskal et al., 2014), and the others are involved in nucleotide metabolism. These extensive changes in the metabolic profiles of *sam1* mutants may reflect the importance of SAM in diverse cellular functions implicated in anti-oxidation, nucleotide metabolism, and pentose pathways.

DISCUSSION

SAM-dependent methylation occurs in a wide variety of cellular compounds, and in the fission yeast, *S. pombe*, one enzyme, the product of the *sam1*$^{+}$ gene, is solely responsible for the synthesis of SAM

	30°C			33°C		
	WT	*sam1-1*	*sam1-3*	WT	*sam1-1*	*sam1-3*
Control	++++	++++	++++	++++	+++	–
25 mM nicotinamide	+++	–	–	+++	–	–
12.5 μg/mL TSA	+++	+++	+++	+++	++	–
4 μg/mL actinomycin D	++	–	–	+++	–	–
4 mM HU	++	++	++	+++	+	–
8 μg/mL phleomycin	+++	+++	+++	+++	±	–
4 μM CPT	+++	+++	+++	+++	+	–
100 J/m^2 UV	++++	++++	++++	++++	+++	–

Table 1. Summary of Colony Formation Abilities of WT and *sam1* Mutants in the Presence of Various Stress Agents
++++, normal growth; +, slow growth; ±, diminished colony formation; –, no colony formation.
See also Figure S3.

from methionine and ATP. There are ~90 methyltransferase genes in the genome of *S. pombe*, so these enzymes are the sources of diversity of methylated substrates. In this study, we examined the cellular defects produced by the genetic impairment of SAM synthesis in the fission yeast, *S. pombe*, using five *sam1* mutants that produced the ts phenotype. Two of them, moderate *sam1-1* and severe *sam1-3*, were further investigated. Both mutants showed Sam1 protein instability, and a great decline of SAM and SAH, whereas increased methionine was observed at the restrictive temperature. As expected, the degree of histone H3 K4 methylation was diminished at the restrictive temperature. The ts phenotype was suppressed by the presence of choline at the semi-restrictive and restrictive temperatures. Exogenous choline, containing three methyl groups, may relieve the ts phenotype by suppressing the defect of PC synthesis and/or reducing the required amount of SAM for cell proliferation. The findings, indeed, indicated that *sam1* mutations cause deterioration of a wide spectrum of methylation reactions.

sam1 mutants showed diverse phenotypes. Two *sam1* mutants (*sam1-1, sam1-3*) are hypersensitive to drugs such as nicotinamide, actinomycin D, HU, phleomycin, and CPT. Considering these drug sensitivities, broad cellular functions implicating methylation seem to necessitate Sam1 enzyme. In addition, rapamycin relieved the defects of *sam1* mutants in both proliferative and quiescence phases. A possible explanation is that the TOR signaling regulates Sam1 via direct or indirect phosphorylation as rapamycin attenuates TOR kinase. Another possibility is that rapamycin, perhaps through TOR kinase, alters methyltransferase activity to give priority to methylation reactions essential to growth. We also identified 12 other groups of ts mutants that were rescued by rapamycin (Sajiki et al., 2018); thus, perhaps Sam1 with some methyltransferases, composes an additional group. According to the report proposing that rapamycin re-balances TOR activity with the activities of identified gene products (Sajiki et al., 2018), the balance between TOR kinase and Sam1 appears important for cell proliferation, and severe impairment of the balance blocks cell growth. The detailed mechanism of this rapamycin-induced rescue should be the subject of further investigation.

Mutations in the *S. pombe sam1* gene affected cell growth (cell size increase) and cell cycle progression at two transition points: the G2/M transition in vegetative culture and the G1/S transition after release from nitrogen-starvation-induced G0 phase. Since fission yeast cells need to increase their size to a critical threshold to pass these two regulatory points (Nurse and Thuriaux, 1977; Nurse, 1975; Shiozaki, 2009), we interpreted our results to mean that a primary defect of mutants resided in cell growth, rather than in the transition of specific cell cycle stages. Our metabolomic analysis of *sam1* mutants suggested that the *sam1* mutation disturbed many metabolic pathways, especially attenuating nucleotide biosynthesis. These metabolic changes appear to cause defects of both cell growth and cell cycle progression, although the precise roles of Sam1 in cell growth remain to be determined.

Sam1 is also required in G0 phase quiescence induced by nitrogen starvation, so Sam1 belongs to a family of SHK gene products, involved in the control of G0 phase, as well as cell growth (Sajiki et al., 2009). *sam1-1*

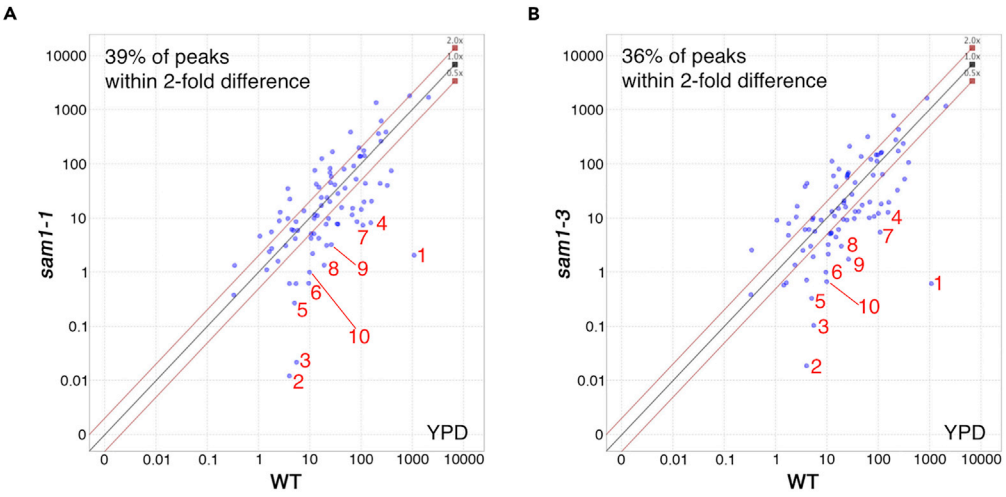

C

	Compound	WT	*sam1-1*	*sam1-3*
1	SAM	1095.98	2.05	0.61
2	PRPP	4.01	0.01	0.02
3	Hercynylcysteine sulfoxide	5.56	0.02	0.10
4	SAH	156.07	8.18	12.71
5	CDP	5.09	0.27	0.33
6	UMP	9.62	0.63	1.00
7	Adenine	109.31	7.34	5.49
8	UDP	19.09	1.34	3.01
9	Sedoheptulose−7−phosphate	9.96	1.00	0.67
10	Pentose−phosphate	26.52	3.23	1.73

Figure 7. Metabolomic Analysis of *sam1* Mutants

(A and B) A scatterplot comparing the normalized peak areas of all identified metabolites in extracts of cells cultured at 36°C for 8 hr in rich YPD medium. WT versus *sam1-1* (A) and WT versus *sam1-3* (B) are shown. Red diagonal lines indicate a 2-fold difference. Most changed compounds are annotated according to the list in (C).

(C) Normalized peak areas of compounds that decreased more than 10-fold in *sam1-1* or *sam1-3* compared with WT. See also Table S1.

lost viability at 26°C in G0 phase, whereas *sam1-3* did not. Why is *sam1-1* more sensitive to this condition than *sam1-3* although the ts phenotype of *sam1-1* was less severe in vegetative culture? One reason is that *sam1-1* seems more defective at 26°C as the SAM content of *sam1-1* is about half of *sam1-3* at 26°C (Figure 2C, 0 hr) and the doubling time of *sam1-1* (3.4 hr) is longer than that of *sam1-3* (3.2 hr) at 26°C. It is also possible that Sam1 protein is differently regulated in G0 phase, as the mutant Sam1 protein level in G0 phase was lower in *sam1-1* than in *sam1-3* (Figure 4E), contrary to the case in vegetative culture. In G0 phase, the level of SAM increases (Shimanuki et al., 2013), and nitrogen sources are recycled for the degradation and synthesis of nucleic acids, proteins, and other nitrogen-containing substrates. Hence, methylated compounds may be central to recycling of nitrogen-containing metabolites.

We isolated and characterized fission yeast ts mutants for the SAM synthetase gene. As the yeast is an excellent model organism for genetic analyses, further study by using these *sam1* mutant strains is expected. However, this single-cell eukaryote does not reveal higher order phenotypes at the level of tissues or organs. In humans, mutations in MAT I/III have been identified as clinical blood variations with hypermethionine and various brain symptoms (Chamberlin et al., 2000; Nagao et al., 2013). Accumulation of methionine seems to be characteristic to all SAM synthetase mutants isolated in different species. In *C. elegans*, S-adenosylmethionine synthetase 1 (SAMS-1) mutants produced enlarged lipid droplets throughout their life cycle and impaired PC synthesis (Ehmke et al., 2014). In both *C. elegans* and *S. pombe*, methyl group-enriched PC is a key metabolite, perhaps because choline is the basic compound for phospholipid

metabolism. In *Arabidopsis thaliana*, a mutation in the S-adenosylmethionine synthetase 3 gene caused high free methionine and decreased lignin (Goto et al., 2002; Shen et al., 2002). In *Neurospora crassa*, mutations of the S-adenosylmethionine synthetase-encoding gene has been identified as an allele resistant to the toxic methionine analog, ethionine (Barra et al., 1996). Taken together, although the phenotypes of different organisms are not universally understood, except for the abundance of methionine, further study of SAM synthetase mutants may open a new avenue to understand the dynamic metabolic regulation of methylation-related biological events, which may be quite complex.

METHODS

All methods can be found in the accompanying Transparent Methods supplemental file.

SUPPLEMENTAL INFORMATION

Supplemental Information includes Transparent Methods, three figures, and one table and can be found with this article online at https://doi.org/10.1016/j.isci.2018.06.011.

ACKNOWLEDGMENTS

We thank Dr. Steven Aird for editing the manuscript. We acknowledge the generous support and funding provided by the Okinawa Institute of Science and Technology Graduate University.

AUTHOR CONTRIBUTIONS

T.H. designed the experiments. T.H. and S.M. performed the experiments. T.T. and R.C. performed metabolomic analyses. T.H., S.M., and M.Y. analyzed data and wrote the manuscript.

DECLARATION OF INTERESTS

The authors declare no competing interests.

Received: March 21, 2018
Revised: June 4, 2018
Accepted: June 27, 2018
Published: July 27, 2018

REFERENCES

Bachand, F., and Silver, P.A. (2004). PRMT3 is a ribosomal protein methyltransferase that affects the cellular levels of ribosomal subunits. EMBO J. *23*, 2641–2650.

Barra, J.L., Mautino, M.R., and Rosa, A.L. (1996). A dominant negative effect of eth-1r, a mutant allele of the Neurospora crassa S-adenosylmethionine synthetase-encoding gene conferring resistance to the methionine toxic analogue ethionine. Genetics *144*, 1455–1462.

Bensaude, O. (2011). Inhibiting eukaryotic transcription: which compound to choose? how to evaluate its activity? Transcription *2*, 103–108.

Chamberlin, M.E., Ubagai, T., Mudd, S.H., Thomas, J., Pao, V.Y., Nguyen, T.K., Levy, H.L., Greene, C., Freehauf, C., and Chou, J.Y. (2000). Methionine adenosyltransferase I/III deficiency: novel mutations and clinical variations. Am. J. Hum. Genet. *66*, 347–355.

Chiang, P.K., Gordon, R.K., Tal, J., Zeng, G.C., Doctor, B.P., Pardhasaradhi, K., and McCann, P.P. (1996). S-Adenosylmethionine and methylation. FASEB J. *10*, 471–480.

Ding, W., Smulan, L.J., Hou, N.S., Taubert, S., Watts, J.L., and Walker, A.K. (2015). s-Adenosylmethionine levels govern innate immunity through distinct methylation-dependent pathways. Cell Metab. *22*, 633–645.

Eckert, K.A., and Kunkel, T.A. (1990). High fidelity DNA synthesis by the *Thermus aquaticus* DNA polymerase. Nucleic Acids Res. *18*, 3739–3744.

Ehmke, M., Luthe, K., Schnabel, R., and Döring, F. (2014). S-adenosyl methionine synthetase 1 limits fat storage in *Caenorhabditis elegans*. Genes Nutr. *9*, 386.

Ekwall, K., and Ruusala, T. (1994). Mutations in rik1, clr2, clr3 and clr4 genes asymmetrically derepress the silent mating-type loci in fission yeast. Genetics *136*, 53–64.

Fontecave, M., Atta, M., and Mulliez, E. (2004). S-adenosylmethionine: nothing goes to waste. Trends Biochem. Sci. *29*, 243–249.

Gerke, J., Bayram, Ö., and Braus, G.H. (2012). Fungal S-adenosylmethionine synthetase and the control of development and secondary metabolism in *Aspergillus nidulans*. Fungal Genet. Biol. *49*, 443–454.

González, B., Pajares, M.A., Hermoso, J.A., Guillerm, D., Guillerm, G., and Sanz-Aparicio, J. (2003). Crystal structures of methionine adenosyltransferase complexed with substrates and products reveal the methionine-ATP recognition and give insights into the catalytic mechanism. J. Mol. Biol. *331*, 407–416.

Goto, D.B., Ogi, M., Kijima, F., Kumagai, T., van Werven, F., Onouchi, H., and Naito, S. (2002). A single-nucleotide mutation in a gene encoding S-adenosylmethionine synthetase is associated with methionine over-accumulation phenotype in Arabidopsis thaliana. Genes Genet. Syst. *77*, 89–95.

Hayashi, K., Ogiyama, Y., Yokomi, K., Nakagawa, T., Kaino, T., and Kawamukai, M. (2014a). Functional conservation of coenzyme Q biosynthetic genes among yeasts, plants, and humans. PLoS One *9*, e99038.

Hayashi, T., Ebe, M., Nagao, K., Kokubu, A., Sajiki, K., and Yanagida, M. (2014b). Schizosaccharomyces pombe centromere protein Mis19 links Mis16 and Mis18 to recruit CENP-A through interacting with NMD factors and the SWI/SNF complex. Genes Cells *19*, 541–554.

Hayashi, T., Hatanaka, M., Nagao, K., Nakaseko, Y., Kanoh, J., Kokubu, A., Ebe, M., and Yanagida, M. (2007). Rapamycin sensitivity of the Schizosaccharomyces pombe tor2 mutant and

organization of two highly phosphorylated TOR complexes by specific and common subunits. Genes Cells *12*, 1357–1370.

Hilti, N., Gräub, R., Jörg, M., Arnold, P., Schweingruber, A.M., and Schweingruber, M.E. (2000). Gene sam1 encoding adenosylmethionine synthetase: effects of its expression in the fission yeast Schizosaccharomyces pombe. Yeast *16*, 1–10.

Hoffman, C.S., Wood, V., and Fantes, P.A. (2015). An ancient yeast for young geneticists: a primer on the Schizosaccharomyces pombe model system. Genetics *201*, 403–423.

Iwaki, T., Iefuji, H., Hiraga, Y., Hosomi, A., Morita, T., Giga-Hama, Y., and Takegawa, K. (2008). Multiple functions of ergosterol in the fission yeast Schizosaccharomyces pombe. Microbiology *154*, 830–841.

Kanipes, M.I., Hill, J.E., and Henry, S.A. (1998). The *Schizosaccharomyces pombe* cho1+ gene encodes a phospholipid methyltransferase. Genetics *150*, 553–562.

Kennedy, B.K., and Lamming, D.W. (2016). The mechanistic target of rapamycin: the grand ConducTOR of metabolism and aging. Cell Metab. *23*, 990–1003.

Kent, C. (1995). Eukaryotic phospholipid biosynthesis. Annu. Rev. Biochem. *64*, 315–343.

Kim, D.-U., Hayles, J., Kim, D., Wood, V., Park, H.-O., Won, M., Yoo, H.-S., Duhig, T., Nam, M., Palmer, G., et al. (2010). Analysis of a genome-wide set of gene deletions in the fission yeast *Schizosaccharomyces pombe*. Nat. Biotechnol. *28*, 617–623.

Li, W., Han, Y., Tao, F., and Chong, K. (2011). Knockdown of SAMS genes encoding S-adenosyl-l-methionine synthetases causes methylation alterations of DNAs and histones and leads to late flowering in rice. J. Plant Physiol. *168*, 1837–1843.

Loenen, W.A.M. (2006). S-adenosylmethionine: jack of all trades and master of everything? Biochem. Soc. Trans. *34*, 330–333.

Moore, C.W. (1988). Internucleosomal cleavage and chromosomal degradation by bleomycin and phleomycin in yeast. Cancer Res. *48*, 6837–6843.

Morris, S.A., Shibata, Y., Noma, K.-I., Tsukamoto, Y., Warren, E., Temple, B., Grewal, S.I.S., and Strahl, B.D. (2005). Histone H3 K36 methylation is associated with transcription elongation in Schizosaccharomyces pombe. Eukaryot. Cell *4*, 1446–1454.

Nagao, M., Tanaka, T., and Furujo, M. (2013). Spectrum of mutations associated with methionine adenosyltransferase I/III deficiency among individuals identified during newborn screening in Japan. Mol. Genet. Metab. *110*, 460–464.

Noga, A.A., Stead, L.M., Zhao, Y., Brosnan, M.E., Brosnan, J.T., and Vance, D.E. (2003). Plasma homocysteine is regulated by phospholipid methylation. J. Biol. Chem. *278*, 5952–5955.

Nurse, P., and Thuriaux, P. (1977). Controls over the timing of DNA replication during the cell cycle of fission yeast. Exp. Cell Res. *107*, 365–375.

Nurse, P. (1975). Genetic control of cell size at cell division in yeast. Nature *256*, 547–551.

Nurse, P., Thuriaux, P., and Nasmyth, K. (1976). Genetic control of the cell division cycle in the fission yeast Schizosaccharomyces pombe. Mol. Gen. Genet. *146*, 167–178.

Obata, F., and Miura, M. (2015). Enhancing S-adenosyl-methionine catabolism extends Drosophila lifespan. Nat. Commun. *6*, 8332.

Pegg, A.E., and Casero, R.A. (2011). Current status of the polyamine research field. Methods Mol. Biol. *720*, 3–35.

Pluskal, T., Nakamura, T., Villar-Briones, A., and Yanagida, M. (2010). Metabolic profiling of the fission yeast S. pombe: quantification of compounds under different temperatures and genetic perturbation. Mol. Biosyst. *6*, 182–198.

Pluskal, T., Ueno, M., and Yanagida, M. (2014). Genetic and metabolomic dissection of the ergothioneine and selenoneine biosynthetic pathway in the fission yeast, S. pombe, and construction of an overproduction system. PLoS One *9*, e97774.

Pommier, Y. (2006). Topoisomerase I inhibitors: camptothecins and beyond. Nat. Rev. Cancer *6*, 789–802.

Ramani, K., and Lu, S.C. (2017). Methionine adenosyltransferases in liver health and diseases. Liver Res. *1*, 103–111.

Sajiki, K., Hatanaka, M., Nakamura, T., Takeda, K., Shimanuki, M., Yoshida, T., Hanyu, Y., Hayashi, T., Nakaseko, Y., and Yanagida, M. (2009). Genetic control of cellular quiescence in S. pombe. J. Cell Sci. *122*, 1418–1429.

Sajiki, K., Tahara, Y., Villar-Briones, A., Pluskal, T., Teruya, T., Mori, A., Hatanaka, M., Ebe, M., Nakamura, T., Aoki, K., et al. (2018). Genetic defects in SAPK signalling, chromatin regulation, vesicle transport and CoA-related lipid metabolism are rescued by rapamycin in fission yeast. Open Biol. *8*, 170261.

Sanders, S.L., Portoso, M., Mata, J., Bähler, J., Allshire, R.C., and Kouzarides, T. (2004). Methylation of histone H4 lysine 20 controls recruitment of Crb2 to sites of DNA damage. Cell *119*, 603–614.

Sauve, A.A., Wolberger, C., Schramm, V.L., and Boeke, J.D. (2006). The biochemistry of sirtuins. Annu. Rev. Biochem. *75*, 435–465.

Shen, B., Li, C., and Tarczynski, M.C. (2002). High free-methionine and decreased lignin content result from a mutation in the Arabidopsis S-adenosyl-L-methionine synthetase 3 gene. Plant J. *29*, 371–380.

Shimanuki, M., Chung, S.-Y., Chikashige, Y., Kawasaki, Y., Uehara, L., Tsutsumi, C., Hatanaka, M., Hiraoka, Y., Nagao, K., and Yanagida, M. (2007). Two-step, extensive alterations in the transcriptome from G0 arrest to cell division in *Schizosaccharomyces pombe*. Genes Cells *12*, 677–692.

Shimanuki, M., Uehara, L., Pluskal, T., Yoshida, T., Kokubu, A., Kawasaki, Y., and Yanagida, M. (2013). Klf1, a C2H2 zinc finger-transcription factor, is required for cell wall maintenance during long-term quiescence in differentiated G0 phase. PLoS One *8*, e78545.

Shiozaki, K. (2009). Nutrition-minded cell cycle. Sci. Signal. *2*, pe74.

Shirai, A., Sadaie, M., Shinmyozu, K., and Nakayama, J. (2010). Methylation of ribosomal protein L42 regulates ribosomal function and stress-adapted cell growth. J. Biol. Chem. *285*, 22448–22460.

Singh, A., and Xu, Y.J. (2016). The cell killing mechanisms of hydroxyurea. Genes (Basel) *7*, 99.

Stead, L.M., Brosnan, J.T., Brosnan, M.E., Vance, D.E., and Jacobs, R.L. (2006). Is it time to reevaluate methyl balance in humans? Am. J. Clin. Nutr. *83*, 5–10.

Su, S.S., Tanaka, Y., Samejima, I., Tanaka, K., and Yanagida, M. (1996). A nitrogen starvation-induced dormant G0 state in fission yeast: the establishment from uncommitted G1 state and its delay for return to proliferation. J. Cell Sci. *109*, 1347–1357.

Thomas, D., and Surdin-Kerjan, Y. (1991). The synthesis of the two S-adenosyl-methionine synthetases is differently regulated in *Saccharomyces cerevisiae*. Mol. Gen. Genet. *226*, 224–232.

Thon, G., Cohen, A., and Klar, A.J. (1994). Three additional linkage groups that repress transcription and meiotic recombination in the mating-type region of Schizosaccharomyces pombe. Genetics *138*, 29–38.

Wei, Y., and Newman, E.B. (2002). Studies on the role of the metK gene product of Escherichia coli K-12. Mol. Microbiol. *43*, 1651–1656.

Wood, V., Harris, M.A., McDowall, M.D., Rutherford, K., Vaughan, B.W., Staines, D.M., Aslett, M., Lock, A., Bähler, J., Kersey, P.J., et al. (2012). PomBase: a comprehensive online resource for fission yeast. Nucleic Acids Res. *40*, D695–D699.

Yanagida, M. (2002). The model unicellular eukaryote, Schizosaccharomyces pombe. Genome Biol. *3*, COMMENT2003.

Ye, C., Sutter, B.M., Wang, Y., Kuang, Z., and Tu, B.P. (2017). A metabolic function for phospholipid and histone methylation. Mol. Cell *66*, 180–193.e8.

Yoshida, M., Horinouchi, S., and Beppu, T. (1995). Trichostatin A and trapoxin: novel chemical probes for the role of histone acetylation in chromatin structure and function. Bioessays *17*, 423–430.

ISCI, Volume *5*

Supplemental Information

S-Adenosylmethionine Synthetase Is Required for Cell Growth, Maintenance of G0 Phase, and Termination of Quiescence in Fission Yeast

Takeshi Hayashi, Takayuki Teruya, Romanas Chaleckis, Susumu Morigasaki, and Mitsuhiro Yanagida

Figure S1

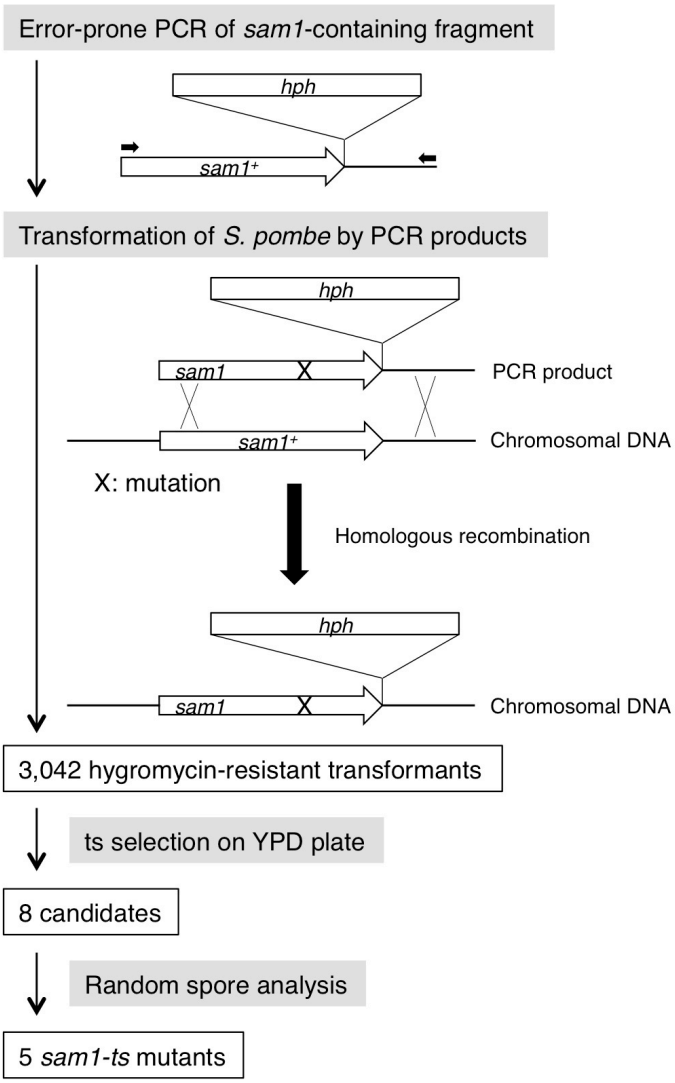

Figure S1. Screening procedures for ts *sam1* mutants, Related to Figure 1

Five ts mutants of *sam1* were identified after screening more than 3,000 hygromycin-resistant transformants.

Figure S2

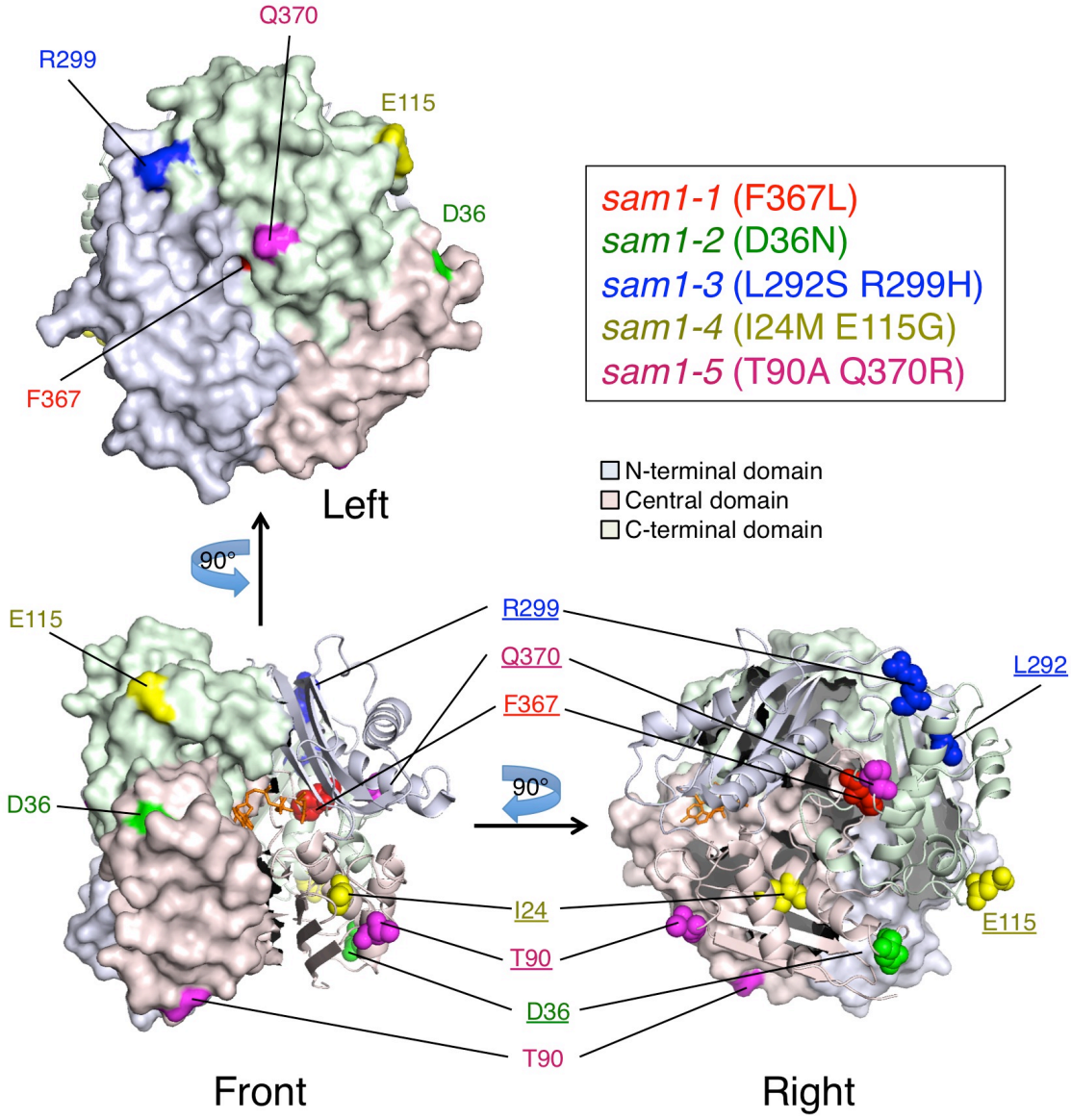

Figure S2. Locations of mutations of *sam1* mutants in the three-dimensional structure, Related to Figure 1

The three-dimensional structure of a homodimer of rat liver MAT, the orthologue of Sam1, is depicted with the positions of amino acids mutated in *sam1* mutants in three orientations. Subunits in the dimer appear as cartoon (monomer A) and molecular surface (monomer B), and N-terminal, central, and C-terminal domains of each subunit are colored light blue, light pink, and light green, respectively. The substrates, ATP and methionine, are represented as orange-colored sticks. Mutated amino acids in *sam1* mutants are colored red (*sam1-1*), green (*sam1-2*), blue (*sam1-3*), yellow (*sam1-4*), and

magenta (*sam1-5*), and labeled with amino acid residue numbers adapted for *S. pombe* Sam1. Amino acid residue numbers of monomer A are underlined. D36, T90, E115, R299, F367 and Q370 are at solvent-exposed surfaces of the dimer, whereas I24 and L292 are not.

Figure S3

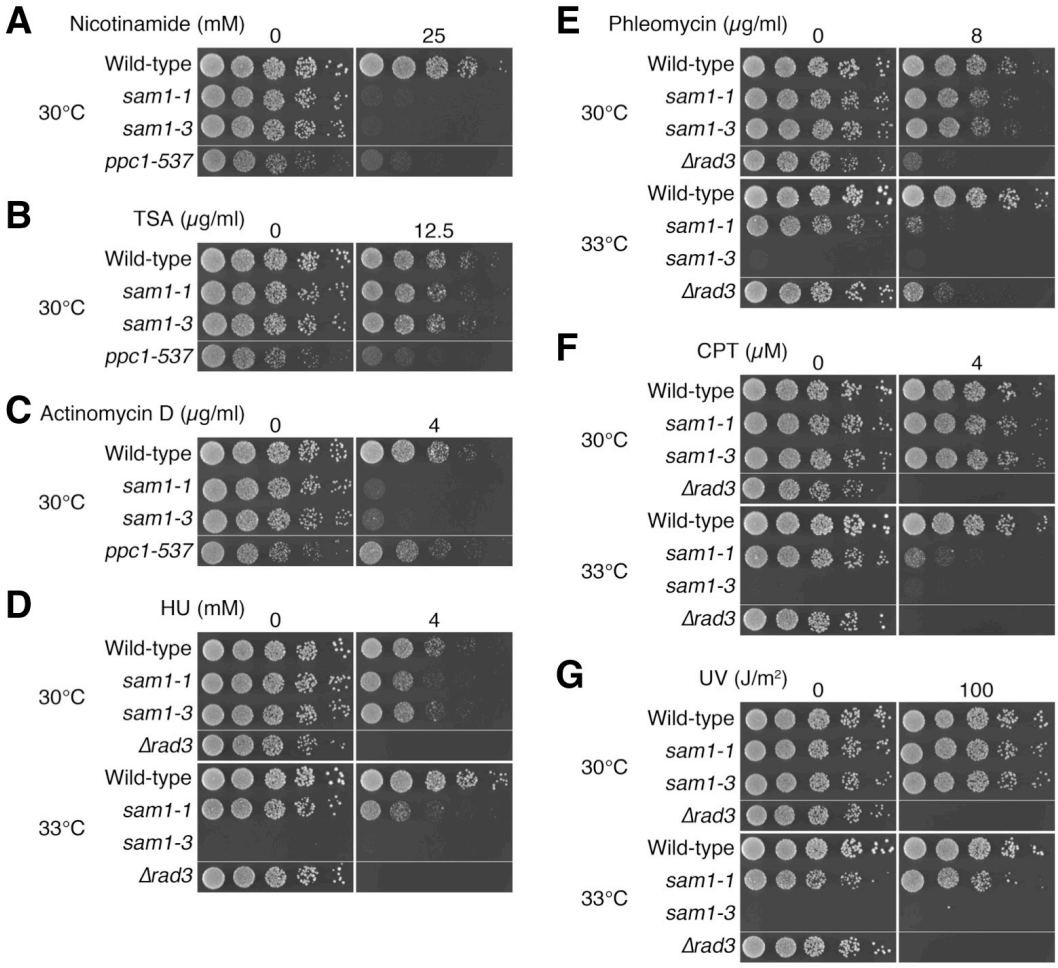

Figure S3. *sam1* mutants are sensitive to nicotinamide, actinomycin D, hydroxyurea, phleomycin and camptothecin, Related to Table 1

sam1-1 and *sam1-3* were spotted on YPD plates in the presence or absence of nicotinamide (A), trichostatin A (B), actinomycin D (C), hydroxyurea (D), phleomycin (E), camptothecin (F), and ultraviolet irradiation (G), and then incubated at the indicated temperatures for 2–3 days. Wild-type, *ppc1-537* and Δ*rad3* were used as controls.

Transparent Methods

Strains

The *S. pombe* strains used in this study are listed below.

Strain	**Genotype**
972	h^-
THO80	h^- *sam1-1[hph]*
THO48	h^- *sam1-2[hph]*
THO116	h^- *sam1-3[hph]*
THO50	h^- *sam1-4[hph]*
THO51	h^- *sam1-5[hph]*
THO55	h^- *sam1-L292S[hph]*
THO56	h^- *sam1-R299H[hph]*
THO52	h^- *sam1-I24M[hph]*
THO54	h^- *sam1-E115G[hph]*
THO53	h^- *sam1-T90A[hph]*
THO57	h^- *sam1-Q370R[hph]*
THO43	*h- leu1 sam1-1[hph]*
THO415	*h- leu1 sam1-3[hph]*
THO3	h^- *sam1-FLAG[hph]*
THO289	h^+ *lys1*$^+$*:nda2p-atb2-GFP cut11-mCherry[nat]*
THO367	h^- *sam1-3[hph] lys1*$^+$*:nda2p-atb2-GFP cut11-mCherry[nat]*
TH2F81	h^- *tor2-287*
THO144	h^- *ppc1-537*
THO100	*ura4* Δ*rad3::ura4*$^+$

Media and general techniques

Growth media and basic methods for *S. pombe* were described (Forsburg and Rhind, 2006; Sherman, 2002). YPD (rich medium) and EMM2 (synthetic minimal medium) were used for cultivation of fission yeast. Nitrogen-starved G0 cells were prepared according to procedures previously described (Su et al., 1996). Briefly, cells exponentially grown in EMM2 to a density of 2×10^6 cells/mL at 26 °C were harvested by vacuum filtration using a nitrocellulose membrane (0.45 μm pore size), washed in

EMM2-N (EMM2 lacking a nitrogen source) once on the membrane, and then re-suspended in EMM2-N at a concentration of 2×10^6 cells/mL and incubated at 26°C for 24 hr. Cells were counted using a Sysmex CDA-500 particle analyzer.

Construction of yeast strains

To tag endogenous *sam1*$^+$ with FLAG, the termination codon of the *sam1*$^+$ gene was changed to the NotI site to incorporate 3FLAG, and was cloned into the pFA6a-hphMX6 derivative plasmid (Hentges et al., 2005), followed by integration into the endogenous *sam1* locus. Correct integration was confirmed by PCR. A similar strategy was used to tag endogenous *cut11*$^+$ with mCherry using the *natMX6* marker (Hentges et al., 2005). The resulting strain expressing Cut11-mCherry was crossed with the strain expressing α-tubulin-GFP (Nakazawa et al., 2016) to obtain strains expressing both α-tubulin-GFP and Cut11-mCherry.

Isolation of ts alleles of *sam1*

Error-prone PCR was performed as described previously (Hayashi et al., 2014). Briefly, the *sam1*$^+$ gene was cloned into the pFA6a-hphMX6 derivative plasmid, and the fused DNA fragment containing the *sam1*$^+$ ORF, the *hph* marker gene and the 0.5-kb downstream sequence of *sam1*$^+$ ORF was amplified by PCR in the presence of increased $MgCl_2$ (8 mM), which significantly reduced the fidelity of polymerization and produced mutated gene fragments (Eckert and Kunkel, 1990). Amplified fragments were used for transformation of wild-type 972 cells. Hygromycin-resistant clones were selected at 26°C and then tested for growth at 36°C on YPD. Mutation sites in isolated strains were determined by sequencing the genomic *sam1* region after PCR amplification. Subsequently, mutations were introduced into the wild-type strain by site-directed mutagenesis, and temperature sensitivity of the resulting integrant strains was examined for reproducibility. The image of mutation sites in the three-dimensional structure was made using the molecular visualization system, PyMOL (Schrödinger, LLC). The structure of a homodimer of rat liver MAT was obtained from the RCSB Protein Data Bank (https://www.rcsb.org/structure/1O9T).

Metabolite analysis

Metabolomic analysis was performed as previously described (Pluskal and

Yanagida, 2016; Pluskal et al., 2010b). Cells from liquid cultures (40 mL/sample, 5.0 × 10^6 cells/mL) were collected and immediately quenched in 25 mL of -40°C methanol. Cells were harvested by centrifugation at -20°C and internal standards (10 nmol of HEPES and PIPES) were added to each sample. Cells were disrupted using a Multi-Beads Shocker (Yasui Kikai) in 500 µL of 50% methanol. Proteins were removed by filtering on an Amicon Ultra 10-kDa cut-off filter (Millipore) and samples were concentrated by vacuum evaporation. Finally, each sample was re-suspended in 40 µL of 50% acetonitrile and 1 µL was used for LS-MS analysis using a Paradigm MS4 HPLC system (Michrom Bioresources) coupled to an LTQ Orbitrap mass spectrometer (Thermo Fisher Scientific). Peak areas of metabolites of interest were measured using MZmine 2 software (Pluskal et al., 2010a) and normalized by the peak areas of spiked internal standards. Among detected peaks, 86 metabolites were identified by comparing their m/z values and retention times with pure standards. Glycerophosphoethanolamine and hercynylcysteine sulfoxide were identified by their theoretical m/z values and MS/MS fragmentation data.

Immunoblotting

Total protein extracts were prepared using the trichloroacetic acid precipitation method (Nagao et al., 2004). Cell were disrupted using glass beads in 10% trichloroacetic acid. Cell extracts were boiled in LDS sample buffer (Invitrogen) and loaded onto a NuPAGE 4-12% Bis-Tris Protein Gel (Invitrogen). Antibodies used were: anti-FLAG (M2, Sigma-Aldrich), anti-α-tubulin (TAT1, a gift from K. Gull), anti-Histone H3 (Abcam, ab1791), anti-monomethyl histone H3 (Lys4) (MABI0302, Takara), anti-dimethyl histone H3 (Lys4) (MABI0303, Takara), and anti-trimethyl histone H3 (Lys4) (MABI0304, Takara). Polyclonal antibodies against *S. pombe* Sam1 were prepared by immunizing rabbits using two synthetic peptides (IGYDDSEKGFDYKTC and NTYGTSSKTSAELV) as antigens (SCRUM Inc., Japan).

Microscopy

DAPI staining was performed as described previously (Adachi and Yanagida, 1989). Cells were fixed with 2% glutaraldehyde for 30 min on ice, washed three times with phosphate-buffered saline (PBS), and observed with a fluorescence microscope (BZ9000 or BZ-X710, Keyence, Japan). Cell length was measured using the “Between

2-points" tool of the "Measurement module" in BZ-II Analyzer software (Keyence, Japan). Methanol-fixed cells were used to observe GFP- and mCherry-tagged proteins, as previously described (Hayashi et al., 2004). Cells were harvested by vacuum filtration and fixed by immersion in 100% methanol at -80°C. After 30 min, PBS was added and cells were washed three times with PBS, and observed with a fluorescence microscope. Ten z-axis sections at 0.2 μm intervals were scanned using a DeltaVision system (GE Healthcare). Obtained images were deconvolved and projected on a 2D plane using SoftWoRx software.

FACS analysis

To measure DNA content of cells, flow cytometry was performed as described previously (Su et al., 1996) with minor modifications. 1×10^7 cells were collected, washed with sterile distilled water, and resuspended in ice-cold 70% ethanol, and then kept at 4°C. Cells were subsequently washed with 0.5 ml 50 mM sodium citrate (pH 7.0) and digested with RNase A (1 mg/ml) for 3 hr at 37°C. Cells were stained with propidium iodide (12.5 μg/ml) and analyzed by FACSCalibur (Becton Dickinson).

Supplemental References

Adachi, Y., and Yanagida, M. (1989). Higher order chromosome structure is affected by cold-sensitive mutations in a Schizosaccharomyces pombe gene crm1+ which encodes a 115-kD protein preferentially localized in the nucleus and its periphery. J. Cell Biol. *108*, 1195–1207.

Eckert, K.A., and Kunkel, T.A. (1990). High fidelity DNA synthesis by the Thermus aquaticus DNA polymerase. Nucleic Acids Research *18*, 3739–3744.

Forsburg, S.L., and Rhind, N. (2006). Basic methods for fission yeast. Yeast *23*, 173–183.

Hayashi, T., Ebe, M., Nagao, K., Kokubu, A., Sajiki, K., and Yanagida, M. (2014). Schizosaccharomyces pombe centromere protein Mis19 links Mis16 and Mis18 to recruit CENP-A through interacting with NMD factors and the SWI/SNF complex. Genes Cells *19*, 541–554.

Hayashi, T., Fujita, Y., Iwasaki, O., Adachi, Y., Takahashi, K., and Yanagida, M. (2004). Mis16 and Mis18 are required for CENP-A loading and histone deacetylation at centromeres. Cell *118*, 715–729.

Hentges, P., Van Driessche, B., Tafforeau, L., Vandenhaute, J., and Carr, A.M. (2005). Three novel antibiotic marker cassettes for gene disruption and marker switching in Schizosaccharomyces pombe. Yeast *22*, 1013–1019.

Nagao, K., Adachi, Y., and Yanagida, M. (2004). Separase-mediated cleavage of cohesin at interphase is required for DNA repair. Nature *430*, 1044–1048.

Nakazawa, N., Mehrotra, R., Arakawa, O., and Yanagida, M. (2016). ICRF-193, an anticancer topoisomerase II inhibitor, induces arched telophase spindles that snap, leading to a ploidy increase in fission yeast. Genes Cells *21*, 978–993.

Pluskal, T., and Yanagida, M. (2016). Metabolomic Analysis of Schizosaccharomyces pombe: Sample Preparation, Detection, and Data Interpretation. Cold Spring Harb Protoc *2016*, pdb.top079921.

Pluskal, T., Castillo, S., Villar-Briones, A., and Orešič, M. (2010a). MZmine 2: modular framework for processing, visualizing, and analyzing mass spectrometry-based molecular profile data. BMC Bioinformatics *11*, 395.

Pluskal, T., Nakamura, T., Villar-Briones, A., and Yanagida, M. (2010b). Metabolic profiling of the fission yeast S. pombe: quantification of compounds under different temperatures and genetic perturbation. Mol Biosyst *6*, 182–198.

Sherman, F. (2002). Getting started with yeast. Meth. Enzymol. *350*, 3–41.

Su, S.S., Tanaka, Y., Samejima, I., Tanaka, K., and Yanagida, M. (1996). A nitrogen starvation-induced dormant G0 state in fission yeast: the establishment from uncommitted G1 state and its delay for return to proliferation. J. Cell. Sci. *109*, 1347–1357.